
The Intrinsic Dimension of Images and Its Impact on Learning

Anonymous Author(s)

Affiliation

Address

email

Abstract

1 It is widely believed that natural image data exhibits low-dimensional structure
2 despite being embedded in a high-dimensional pixel space. This idea underlies a
3 common intuition for the success of deep learning and has been exploited for en-
4 hanced regularization and adversarial robustness. In this work, we apply dimension
5 estimation tools to popular datasets and investigate the role of low dimensional
6 structure in neural network learning. We find that common natural image datasets
7 indeed have very low intrinsic dimension relative to the high number of pixels in
8 the images. Additionally, we find that low dimensional datasets are easier for neural
9 networks to learn. We validate our findings by carefully-designed experiments to
10 vary the intrinsic dimension of both synthetic and real data and evaluate its impact
11 on sample complexity.

12 1 Introduction

13 The idea that real-world data distributions can be described by very few variables underpins machine
14 learning research from manifold learning to dimension reduction (Besold & Spokoiny, 2019; Fodor,
15 2002). The number of variables needed to describe a data distribution is known as its *intrinsic*
16 *dimension* (ID). In applications, such as crystallography, computer graphics, and ecology, practitioners
17 depend on data having low intrinsic dimension (Valle & Oganov, 2010; Desbrun et al., 2002;
18 Laughlin, 2014). A variety of deep learning techniques including autoencoders and regularization
19 methods (Gonzalez & Balajewicz, 2018; Zhu et al., 2018) are also motivated by the low-dimensional
20 assumption of data.

21 It is known that dimensionality plays a strong
22 role in learning function approximations and
23 non-linear class boundaries. The exponential
24 cost of learning in high dimensions is easily
25 captured by the trivial case of sampling a func-
26 tion on a cube; in n dimensions, sampling only
27 the cube vertices would require 2^n measure-
28 ments. Similar behaviors emerge in learning
29 theory. It is known that learning a manifold
30 requires a number of samples that grows expo-
31 nentially with the manifold’s intrinsic dimen-
32 sion (Narayanan & Mitter, 2010). Similarly,
33 the number of samples needed to learn a well-
34 conditioned decision boundary between two
35 classes is an exponential function of the intrinsic

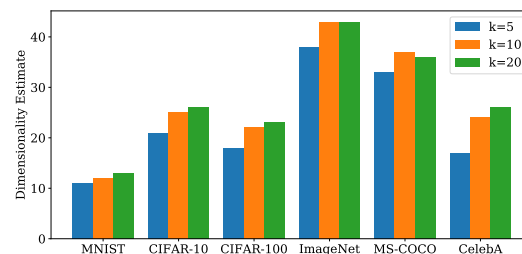


Figure 1: Estimates of the dimensionality of popular datasets obtained using the MLE method with $k = 5, 10, 20$ nearest neighbors (left to right).

36 dimension of the manifold on which the classes lie (Narayanan & Niyogi, 2009). Furthermore, these
37 learning bounds have no dependence on the ambient dimension in which manifold-structured datasets
38 live.

39 In light of the exponentially large sample complexity of learning high-dimensional functions, the
40 seemingly low number of samples needed for neural networks to learn image manifolds strongly
41 suggests that image datasets have extremely low-dimensional structure.. Networks learn complex
42 decision boundaries from small amounts of image data, e.g., ImageNet has no more than 1300 images
43 for each of the 1000 classes. At the same time, Generative adversarial networks are able to learn
44 image “manifolds” from merely a few thousand samples.

45 Despite the established role of low dimensionality in deep learning, little is known about the intrinsic
46 dimension of popular datasets and the impact of dimensionality on the performance of neural networks.
47 We adopt tools from the dimension estimation literature to shed light on dimensionality in settings of
48 interest to the deep learning community. Our contributions are summarized as follows:

- 49 • We verify the reliability of intrinsic dimension estimation on high-dimensional data using
50 generative adversarial networks (GANs), a setting where we can upper-bound the intrinsic
51 dimension of generated data a priori by the dimension of the latent noise vector.
- 52 • We measure the dimensionality of popular datasets such as MNIST, CIFAR-10, and Im-
53 ageNet. In our experiments, we find that natural image datasets whose images contain
54 thousands of pixels can, in fact, be described by orders of magnitude fewer variables. For
55 example, we estimate that ImageNet, despite containing 150K pixels per image, only has an
56 intrinsic dimension between 38 and 43; see Figure 1.
- 57 • We train classifiers on synthetic and real data of various intrinsic dimension and find that this
58 variable correlates closely with the sample complexity for learning. On the other hand, we
59 find that the dimension of the ambient space of the data has little impact on generalization.

60 Our results put experimental weight behind the hypothesis that the unintuitively low dimensionality
61 of natural images is being exploited by deep networks, and suggest that a characterization of this
62 structure is an essential building block for a successful theory of deep learning. A brief review of
63 related work can be found in Appendix A.

64 2 Scalable Estimation of Intrinsic Dimension

65 Given a set of sample points $\mathcal{P} \subset \mathbb{R}^N$, it is common to assume that \mathcal{P} lies on or near a low-
66 dimensional manifold $\mathcal{M} \subseteq \mathbb{R}^N$ of intrinsic dimension $\dim(\mathcal{M}) = D \ll N$. We implemented a
67 scalable version of the popular Maximum Likelihood Estimator (MLE) of Levina & Bickel (2004);
68 for further information on dimension estimation, see (Kim et al., 2019) and references therein.

69 2.1 Validation on Synthetic Data

70 Towards a principled application of ID estimates on images, we begin by validating that MLE methods
71 can generate accurate dimensionality estimates for complex image manifolds. We generate image
72 datasets using generative models for which the intrinsic dimensionality is bounded. We believe such
73 validations are essential to put recent findings in perspective (Gong et al., 2019; Ansuini et al., 2019).

74 We use the BigGAN variant with 128 latent entries and outputs of size $128 \times 128 \times 3$ trained on the
75 ImageNet dataset (Deng et al., 2009) to generate datasets with various number of images, where we
76 fix most entries of the latent vectors to zero leaving only n free entries to be chosen at random. As we
77 increase the number of free entries, we expect the intrinsic dimension to increase but not to exceed n ;
78 see Appendix C.1 for further discussions.

79 In particular, we create several synthetic datasets of varying intrinsic dimensionality using the
80 ImageNet class, `basenji`, and check if the estimates match our expectation. As seen in Figure 5, we
81 observe increasing diversity with increasing intrinsic dimension. In Figure 6, we show convergence
82 of the MLE estimate on `basenji` data with dimension bounded above by 10. We also observe that
83 the estimates can be sensitive to the choice of k as discussed in prior works; see Appendix C.2 for
84 additional GAN classes. In addition, we evaluate the accuracy of averaging a subset of local MLE
85 estimates for large-scale datasets like ImageNet; see Appendix C.3 for details.

Dataset	MNIST	CIFAR-10	CIFAR-100	ImageNet	MS-COCO	CelebA
MLE ($k=5$)	11	21	18	38	33	17
MLE ($k=10$)	12	25	22	43	37	24
MLE ($k=20$)	13	26	23	43	36	26
SOTA Accuracy	99.84	99.37	93.51	88.5	-	-

Table 1: The MLE estimates for practical image datasets, and the state-of-the-art test-set image classification accuracy (for classification problems only) for these datasets.

86 2.2 The Intrinsic Dimension of Popular Datasets

87 In this section, we measure the intrinsic dimensions of a number of popular datasets including
88 MNIST (Deng, 2012), CIFAR-10 and CIFAR-100 (Krizhevsky et al., 2009), ImageNet (Deng et al.,
89 2009), MS-COCO (Lin et al., 2014), and CelebA (Liu et al., 2015). Using three different parameter
90 settings for MLE, we find that the ID is indeed much smaller than the number of pixels; see Table 2.2.
91 Notice that the rank order of datasets by dimension does not depend on the choice of k . A comparison
92 of state-of-the-art classification accuracy on each respective dataset¹ with the dimension estimates
93 suggests a negative correlation between the intrinsic dimension and test accuracy. In the next section,
94 we take a closer look at this phenomenon through a series of dedicated experiments.

95 3 Intrinsic Dimension and Generalization

96 Narayanan & Mitter (2010) have establish that learning a manifold requires a number of samples that
97 grows exponentially with the manifold’s intrinsic dimension, but the required number of samples is
98 independent of the extrinsic dimension. We leverage dimension estimation tools to empirically verify
99 these theoretical findings by a family of binary classification problems defined on both synthetic and
100 real datasets of varying ID. We then train classifiers on these datasets and measure test accuracy. In
101 these experiments, we find that classification problems on data of lower intrinsic-dimensionality are
102 easier to solve.

103 3.1 Synthetic data: Sample complexity depends on intrinsic (not extrinsic) dimensionality

104 The synthetic GAN data generation technique described in Section B provides a unique opportunity
105 to test the relationship between generalization and intrinsic/extrinsic dimensionality on images. By
106 creating datasets with controlled intrinsic dimensionality, we may compare their *sample complexity*,
107 that is the number of samples required to obtain a given level of test error. Specifically we test the
108 following two hypotheses (1) data of lower intrinsic dimensionality has lower sample complexity
109 than that of higher intrinsic dimensionality and (2) extrinsic dimensionality is irrelevant for sample
110 complexity.

111 To investigate hypothesis (1), we create four synthetic datasets of varying intrinsic dimensionality:
112 16, 32, 64, 128, *fixed* extrinsic dimensionality: $3 \times 128 \times 128$, and two classes: `basenji` and `beagle`.
113 For each dataset we fix a test set of size $N = 1700$. For all experiments, we use the ResNet-18
114 (width=64) architecture (He et al., 2016). We then train models until they fit their entire training
115 set with increasing amounts of training samples and measure the test error. We show these results
116 in Figure 2. Observing the varying rates of growth, we see that data of higher intrinsic dimension
117 requires more samples to achieve a given test error.

118 For hypothesis (2), we carry out the same experiment with the roles of intrinsic and extrinsic dimension
119 switched. We create four synthetic datasets of varying *extrinsic* dimensionality by resizing the images
120 with nearest-neighbor interpolation. Specifically we create 6 datasets of square, 3-channel images
121 of sizes 16, 32, 64, 128, 256, *fixed* intrinsic dimensionality of size 128, and all other experimental
122 details the same. We show these results in Figure 3. Observing the lack of variable growth rates, we
123 see that extrinsic dimension has little to no effect on sample complexity.

124 We conclude by noting that, to the best of our knowledge, this is the first such experimental result
125 to demonstrate that *intrinsic but not extrinsic dimensionality matters for the generalization of deep*
126 *networks*.

¹Values from <https://paperswithcode.com/task/image-classification>.

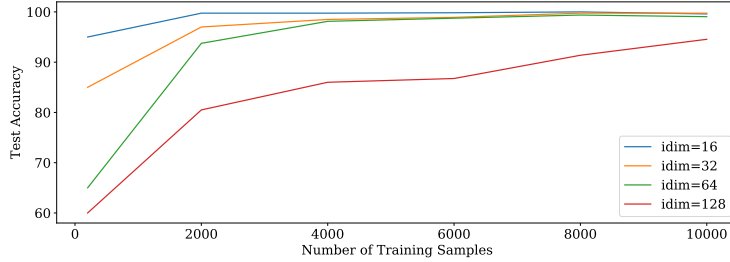


Figure 2: Sample complexity of synthetic datasets of varying intrinsic dimensionality.

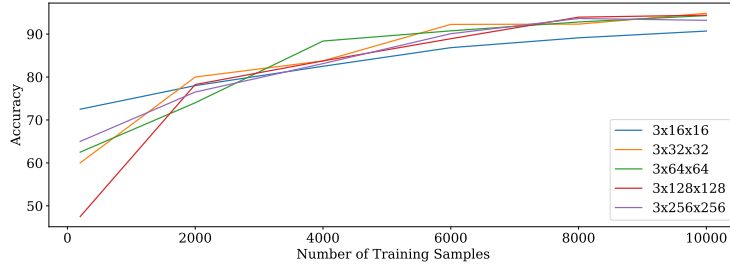


Figure 3: Sample complexity of synthetic datasets of varying extrinsic dimensionality.

127 **3.2 Real data: Adding noise changes dimensionality and affects generalization**

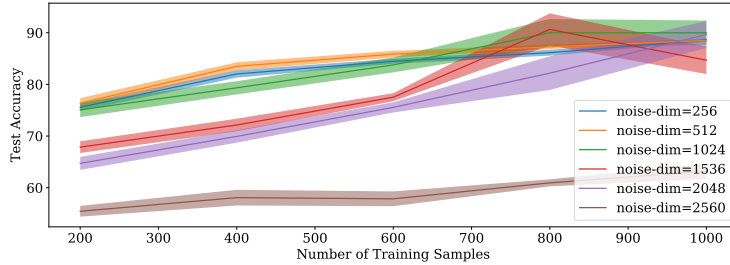


Figure 4: Sample complexity of noisy datasets.

128 For real data, we evaluate the impact of ID on generalization by: (1) increasing the ID of a dataset by
 129 varying amount of additive noise to each image and comparing the test accuracy; (2) comparing the
 130 test accuracy of different datasets with different IDs. We defer (2) to Appendix D.

131 By adding noise to the images of a *real* dataset, we are leveraging the fact that uniformly sampled
 132 noise in $[0, 1]^d$ has dimension d . We thus add independent noise, drawn uniformly from a fixed
 133 randomly oriented d -dimensional unit hypercube embedded in pixel space, to each sample in a dataset.
 134 This procedure ensures that the dataset has dimension at least d . Since we have shown these datasets
 135 have low IDs, this procedure specifically increases ID in most cases. We note that estimation error
 136 may occur when there is an insufficient number of samples required to achieve a proper dimension
 137 estimate. Since the variation in images in a dataset may still be dominated by non-noise directions,
 138 we expect to underestimate the new increased dimensions of these noised datasets.

139 Starting with CIFAR-10 data, we add noise of varying dimensions, where we replace pix-
 140 els at random in the image. We only add noise to an image once to keep the aug-
 141 mented dataset the same size as the original. We use the following noise dimensionalities:
 142 256, 512, 1024, 2048, 2560. The new noised data respectively obtains the following MLE dimension-
 143 ality estimates: 19.7, 30.9, 57.1, 77.8, 110.0, 136.1. We see that intrinsic dimension increases with
 144 increasing noise dimensionality, but dimensionality does not saturate to the maximum true dimension,
 145 likely due to a poverty of samples. We show results on these noisy CIFAR-10 datasets in Figure 4.
 146 We observe sample complexity largely in the same order as intrinsic dimension.

147 References

- 148 Alessio Ansuini, Alessandro Laio, Jakob H Macke, and Davide Zoccolan. Intrinsic dimension of data repre-
149 sentations in deep neural networks. In *Advances in Neural Information Processing Systems*, pp. 6111–6122,
150 2019.
- 151 Franz Besold and Vladimir Spokoiny. Adaptive manifold clustering. *arXiv preprint arXiv:1912.04869*, 2019.
- 152 Andrew Brock, Jeff Donahue, and Karen Simonyan. Large scale GAN training for high fidelity natural image
153 synthesis. *arXiv preprint arXiv:1809.11096*, 2018.
- 154 Gunnar Carlsson, Tigran Ishkhanov, Vin de Silva, and Afra Zomorodian. On the local behavior of spaces of
155 natural images. *International Journal of Computer Vision*, 76(1):1–12, 2008.
- 156 Jia Deng, Wei Dong, Richard Socher, Li-Jia Li, Kai Li, and Li Fei-Fei. ImageNet: A large-scale hierarchical
157 image database. In *2009 IEEE conference on computer vision and pattern recognition*, pp. 248–255. Ieee,
158 2009.
- 159 Li Deng. The MNIST database of handwritten digit images for machine learning research [best of the web].
160 *IEEE Signal Processing Magazine*, 29(6):141–142, 2012.
- 161 Mathieu Desbrun, Mark Meyer, and Pierre Alliez. Intrinsic Parameterizations of Surface Meshes. *Computer
162 Graphics Forum*, 2002.
- 163 David L. Donoho and Carrie Grimes. Image manifolds which are isometric to euclidean space. *Journal of
164 Mathematical Imaging and Vision*, 23(1):5–24, 2005.
- 165 Charles Fefferman, Sanjoy Mitter, and Hariharan Narayanan. Testing the manifold hypothesis. *Journal of the
166 American Mathematical Society*, 29(4):983–1049, 2016.
- 167 Imola K Fodor. A survey of dimension reduction techniques. Technical report, Lawrence Livermore National
168 Lab., CA (US), 2002.
- 169 Sixue Gong, Vishnu Naresh Boddeti, and Anil K Jain. On the intrinsic dimensionality of image representations.
170 In *Proceedings of the IEEE Conference on Computer Vision and Pattern Recognition*, pp. 3987–3996, 2019.
- 171 Francisco J Gonzalez and Maciej Balajewicz. Deep convolutional recurrent autoencoders for learning low-
172 dimensional feature dynamics of fluid systems. *arXiv preprint arXiv:1808.01346*, 2018.
- 173 Kaiming He, Xiangyu Zhang, Shaoqing Ren, and Jian Sun. Deep residual learning for image recognition. In
174 *Proceedings of the IEEE conference on computer vision and pattern recognition*, pp. 770–778, 2016.
- 175 W. Ronny Huang, Zeyad Emam, Micah Goldblum, Liam Fowl, Justin K. Terry, Furong Huang, and Tom
176 Goldstein. Understanding generalization through visualizations, 2019.
- 177 Jisu Kim, Alessandro Rinaldo, and Larry Wasserman. Minimax Rates for Estimating the Dimension of a
178 Manifold. *Journal of Computational Geometry*, 10(1), 2019.
- 179 Alex Krizhevsky, Geoffrey Hinton, et al. Learning multiple layers of features from tiny images. University of
180 Toronto, 2009. Master’s thesis.
- 181 Daniel C. Laughlin. The intrinsic dimensionality of plant traits and its relevance to community assembly. *Journal
182 of Ecology*, 102(1):186–193, 2014.
- 183 Ann B. Lee, Kim S. Pedersen, and David Mumford. The nonlinear statistics of high-contrast patches in natural
184 images. *International Journal of Computer Vision*, 54(1):83–103, 2003.
- 185 Elizaveta Levina and Peter J. Bickel. Maximum likelihood estimation of intrinsic dimension. In *Proceedings of
186 the 17th International Conference on Neural Information Processing Systems, NIPS’04*, pp. 777–784, 2004.
- 187 Tsung-Yi Lin, Michael Maire, Serge Belongie, James Hays, Pietro Perona, Deva Ramanan, Piotr Dollár, and
188 C Lawrence Zitnick. Microsoft COCO: Common objects in context. In *European conference on computer
189 vision*, pp. 740–755. Springer, 2014.
- 190 Ziwei Liu, Ping Luo, Xiaogang Wang, and Xiaoou Tang. Deep learning face attributes in the wild. In *Proceedings
191 of the IEEE international conference on computer vision*, pp. 3730–3738, 2015.
- 192 Hariharan Narayanan and Sanjoy Mitter. Sample complexity of testing the manifold hypothesis. In *Advances in
193 neural information processing systems*, pp. 1786–1794, 2010.

- 194 Hariharan Narayanan and Partha Niyogi. On the sample complexity of learning smooth cuts on a manifold. In
195 *COLT*, 2009.
- 196 Bruno A Olshausen and David J Field. Natural image statistics and efficient coding. *Network: Computation in*
197 *Neural Systems*, 7(2):333–339, 1996.
- 198 Gabriel Peyré. Manifold models for signals and images. *Computer Vision and Image Understanding*, 113(2):
199 249 – 260, 2009.
- 200 Daniel L Ruderman. The statistics of natural images. *Network: Computation in Neural Systems*, 5(4):517–548,
201 1994.
- 202 Mario Valle and Artem R. Oganov. Crystal fingerprint space – a novel paradigm for studying crystal-structure
203 sets. *Acta Crystallographica Section A*, 66(5):507–517, 2010.
- 204 Wei Zhu, Qiang Qiu, Jiaji Huang, Robert Calderbank, Guillermo Sapiro, and Ingrid Daubechies. LDMNet: Low
205 dimensional manifold regularized neural networks. In *The IEEE Conference on Computer Vision and Pattern*
206 *Recognition (CVPR)*, June 2018.

207 A Related Work

208 Early work on efficient image representations emphasized the importance of natural image statistics (Ruderman,
209 1994). It is widely believed that the combination of natural scenes and sensor properties yields very sparse and
210 concentrated image distributions, as has been supported by several empirical studies on image patches (Lee et al.,
211 2003; Donoho & Grimes, 2005; Carlsson et al., 2008). This observation motivated lots of work on efficient
212 coding (Olshausen & Field, 1996) and served as a prior in computer vision (Peyré, 2009). Other work has
213 focused on algorithms for verifying the manifold hypothesis (Fefferman et al., 2016).

214 The generalization literature seeks to understand why some models generalize better from training data to test
215 data than others. One line of work suggests that the loss landscape geometry explains why neural networks
216 generalize well (Huang et al., 2019). Other generalization work predicts that data with low dimension, along
217 with other properties which do not include extrinsic dimension, characterize the generalization difficulty of
218 classification problems (Narayanan & Niyogi, 2009). In the context of deep learning, Gong et al. (2019) found
219 that neural network features are low-dimensional. Ansuini et al. (2019) further found that the intrinsic dimension
220 of features decreases in late layers of neural networks and observed interesting trends in the dimension of
221 features in early layers. Zhu et al. (2018) recently proposed a regularizer derived from the intrinsic dimension of
222 images augmented with their corresponding feature vectors.

223 B Validating Dimension Estimation with Synthetic Data

224 Dimensionality estimates are often applied on “simple” manifolds or toy datasets where the dimensionality is
225 known, and so the accuracy of the methods can be validated. Image manifolds, by contrast, are highly complex,
226 may contain many symmetries and modes, and are of unknown dimension. In principle, there is no reason why
227 MLE-based dimensionality estimates cannot be applied to image datasets. However, because we lack knowledge
228 of the exact dimensionality of image datasets, we cannot directly verify that MLE-based dimensionality estimates
229 scale up to the complexity of image structures.

230 There is an inherent uncertainty in estimating the ID of a given dataset. First, we cannot be sure if the dataset
231 actually resembles a sampling of points on or near a manifold. Second, there are typically no guarantees that the
232 sampling satisfies the conditions assumed by the ID estimators we are using.

233 Towards a principled application of ID estimates to the learning context, we begin by validating that MLE
234 methods can generate accurate dimensionality estimates for complex image structures. We do this by generating
235 image datasets using generative models for which the intrinsic dimensionality is known. We believe such
236 validations are essential to put recent findings in perspective (Gong et al., 2019; Ansuini et al., 2019).

237 **GAN Images.** We use the BigGAN variant with 128 latent entries and outputs of size $128 \times 128 \times 3$ trained
238 on the ImageNet dataset (Deng et al., 2009). Using this GAN, we generate datasets with a varying number of
239 images, where we fix most entries of the latent vectors to zero leaving only n free entries to be chosen at random.
240 As we increase the number of free entries, we expect the intrinsic dimension to increase, and the output can only
241 be at most n -dimensional; see Section C.1 for further discussion.

242 In particular, we create several synthetic datasets of varying intrinsic dimensionality using the ImageNet class,
243 `basenji`, and check if the estimates match our expectation. As seen in Figure 5, we observe increasing diversity
244 with increasing intrinsic dimension. In Figure 6, we show convergence of the MLE estimate on `basenji` data
245 with dimension bounded above by 10. We observe that the estimates can be sensitive to the choice of k as
246 discussed in prior work; see Appendix C.2 for additional GAN classes.

247 **Scaling to large datasets.** We develop a practical approach for estimating the ID of large datasets such as
248 ImageNet. In this approach, we randomly select a fraction α of the dataset as anchors. Then, we evaluate the
249 MLE estimate using only the anchor points, where nearest-neighbors are computed over the entire dataset. Note
250 that, when anchors are chosen randomly, this acceleration has no impact on the expected value of the result. See
251 Appendix C.3 for an evaluation of this approach.

252 As with simpler manifolds, we find that there is some variation in the estimate with the choice of k , with $k = 10$
253 consistently yielding good estimates on this dataset. Despite this variation, it appears that MLE is capable of
254 estimating the dimensionality of this image-structured data within a reasonable margin of error.

255 C Validation of ID Estimates

256 In this section, we present additional discussion results and discussion relevant to the ID estimation and related
257 validation experiments in Section B.

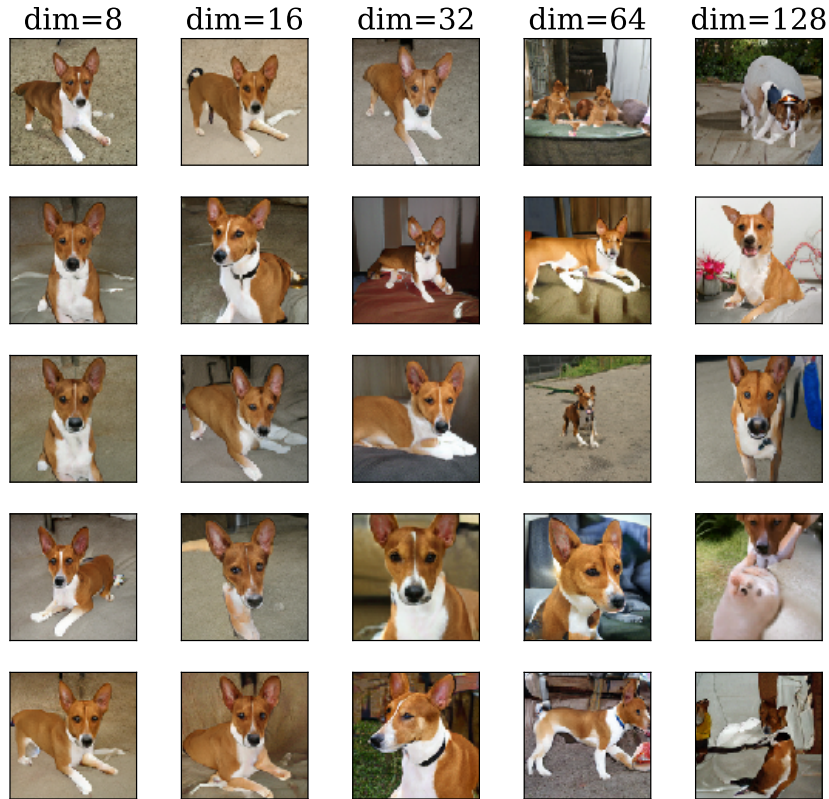


Figure 5: Visualization of basenji GAN samples of varying intrinsic dimension.

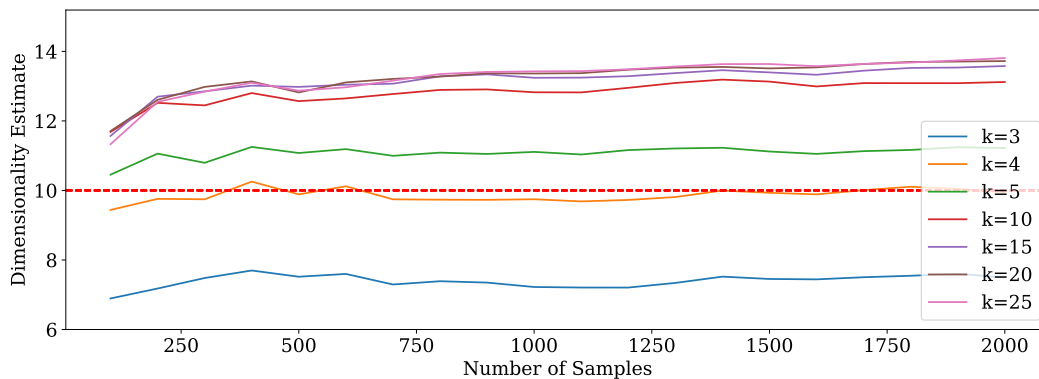


Figure 6: Validation of MLE estimate on synthetic basenji data with $n = 10$ free entries. We observe the estimates to converge around the expected dimensionality of 10.

258 C.1 GAN properties

259 We devise a method for validating ID measurements in a controlled setting using images generated by GANs. To
 260 justify this method, we first note that the image of \mathbb{R}^d under a locally Lipschitz function can be a manifold with
 261 dimension at most d . Then, consider that the BigGAN generator, a convolutional neural network with ReLU
 262 activations, is a function with this property (Brock et al., 2018).

263 Specifically, BigGAN can be written as a composition of linear functions, translations, and ReLU activation
 264 functions. Individually, these operations do not increase dimension, and by a composition property, their
 265 composition cannot increase dimensionality either. The more general fact that the image of \mathbb{R}^d under a locally
 266 Lipschitz function can be a manifold with dimension at most d follows from Sard's theorem.

267 **C.2 Convergence for More GAN Classes**

268 We include additional results on the estimation of ID for synthetic GAN images from various ImageNet classes
 269 with $n = 10$ free entries. As observed earlier in Section B, the MLE estimates are sensitive to the choice of k ,
 270 where we expect the ID to be close to 10 given the way we sample the latent vectors to use for the GAN. We
 271 note that for a number of classes, all choices of k we considered seem to underestimate the ID.

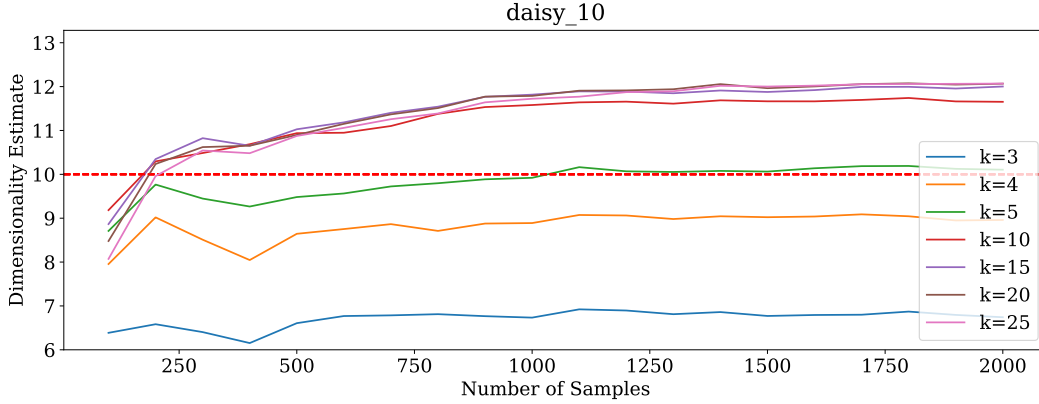


Figure 7: Validation of MLE estimates on synthetic daisy data with 10 free entries.

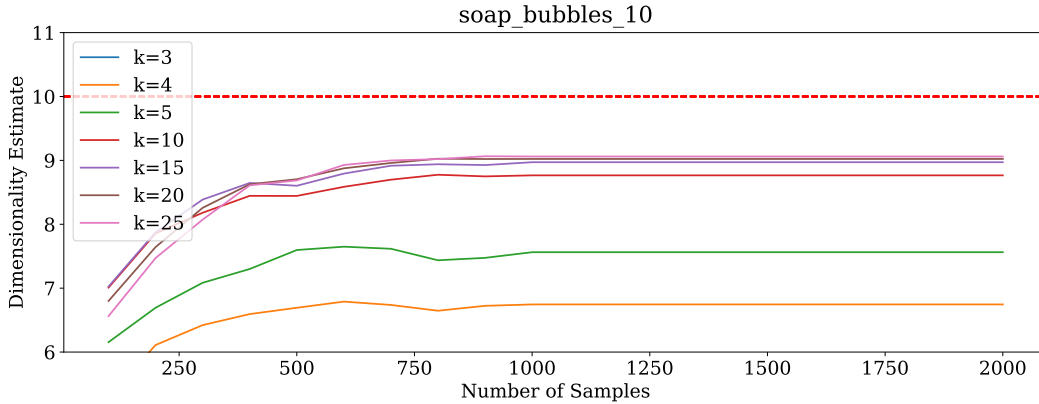


Figure 8: Validation of MLE estimate on synthetic soap-bubbles data with 10 free entries.

272 **C.3 Subsampling for Large Datasets**

273 In Figure 10 we validate the anchor approximation on basenji data of dimension 10 for varying anchor ratio α .
 274 Then, in Figure 11 we validate the anchor approximation on tree-frog data of dimension 32 for varying k
 275 while fixing the anchor ratio at $\alpha = 0.001$.

276 **D Real Data: Intrinsic dimensionality matters for generalization**

277 We examine the sample complexity of binary classification tasks from four common image datasets: MNIST,
 278 SVHN, CIFAR-10, and ImageNet. This case differs from the synthetic case in that we have no control over each
 279 dataset’s intrinsic dimension. Instead, we estimate it via the MLE method discussed in Section 2. To account
 280 for variable difficulty of classes, we randomly sample 5 class pairs from each dataset and run the previously
 281 described sample complexity experiment. Note that these subsets differ from those used in Table 2.2, where the
 282 estimates are taken from the entire dataset and across all classes.

283 On these sampled subsets, we find the following mean MLE estimates ($k = 3$): MNIST $\rightarrow 7.5 \pm 0.2$, SVHN \rightarrow
 284 8.5 ± 0.1 , CIFAR-10 $\rightarrow 11.4 \pm 0.2$, ImageNet $\rightarrow 15.4 \pm 0.8$. We note that these estimates are consistent with
 285 expectation, e.g. MNIST is qualitatively less complex than SVHN and CIFAR-10.

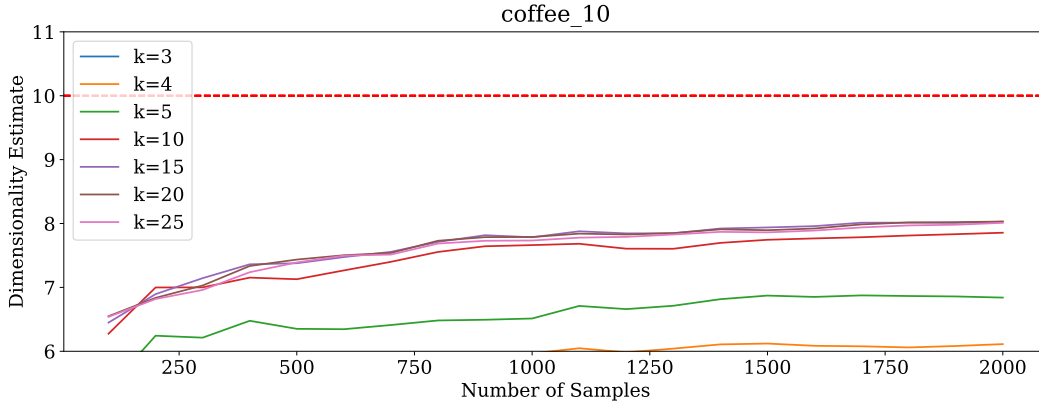


Figure 9: Validation of MLE estimate on synthetic `coffee` data with 10 free entries. Note that the estimates do not converge around the upper bound of 10, which suggests that data generated from this class is not of full dimension.

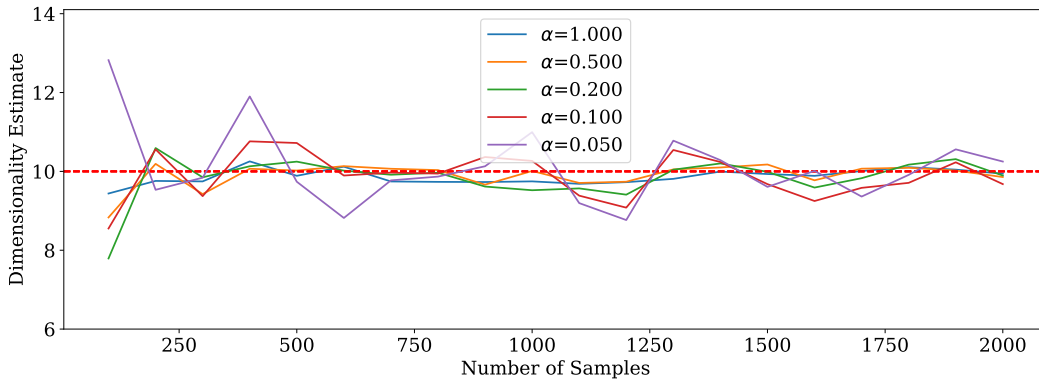


Figure 10: Validation of anchor approximation on `basenji` with 10 free entries.

286 We conduct the same sample complexity experiment as the previous section on the datasets. Because these
 287 datasets are ordinarily of varying extrinsic dimensionality, we resize all to size $32 \times 32 \times 3$ (before applying
 288 MLE). We report results in Figure 12, where we overall observe trends ordered by intrinsic dimensionality
 289 estimate. These results are consistent with expectation of the relative hardness of each dataset. However, there are
 290 some notable differences from the synthetic case. Several unexpected cross-over points exist in the low-sample
 291 regime, and the gap between SVHN and CIFAR-10 is smaller than one may expect based on their estimated
 292 intrinsic dimension.

293 From these observations we conclude that intrinsic dimensionality is indeed relevant to generalization on real
 294 data, but it is not the only feature of data that influences sample complexity.

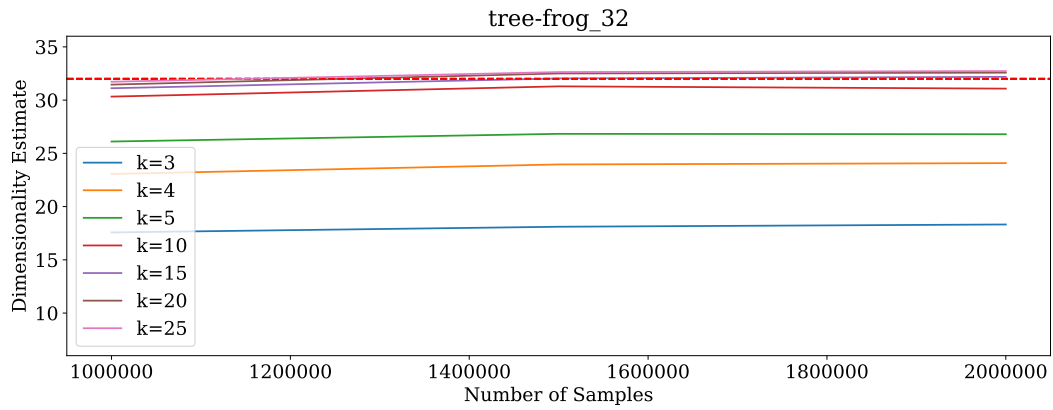


Figure 11: Validation of anchor approximation on *tree-frog* with $n = 32$ free entries.

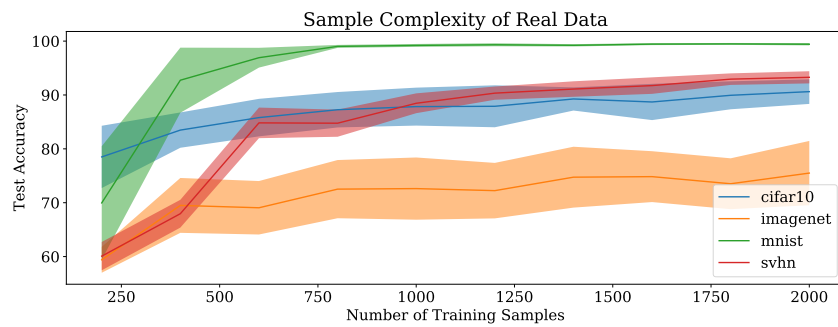


Figure 12: Sample complexity of real datasets.